RESEARCH ARTICLE
Published: 6 July 2026

Volume 13 | Issue 2 | 363-377

OPEN ACCESS

Journal of Daylighting

Journal homepage: www.solarlits.com/jd

Façade Geometry, Orientation, and Window-to-Wall Ratio: An integrated Energy and Daylight performance study for Kathmandu's temperate climate

Prashant Chhetri *

Department of Architecture, Institute of Engineering, Tribhuvan University, Lalitpur, 44700, Nepal

ABSTRACT

Window-to-Wall Ratio (WWR) influences building energy and daylight performance, yet its implications depend on both façade orientation and geometry. In rapidly urbanizing regions lacking energy regulations, WWR decisions are often made without systematic feedback. This study investigates the combined effect of WWR, orientation, and façade geometry on heating, cooling, and daylight performance for residential buildings in Kathmandu's temperate climate. A parametric simulation framework using EnergyPlus and Radiance was developed based on mean room dimensions from 50 surveyed Kathmandu buildings. A total of 360 simulations were evaluated using Energy Use Intensity (EUI), Spatial Daylight Autonomy (sDA), and Spatial Glare Autonomy (sGA). Standardized Regression Coefficients (SRC) were employed to rank the sensitivity of WWR on heating and cooling loads across paired façade configurations, with Spearman's rank correlation validating the monotonic nature of the relationships despite underlying non-linearity. Results reveal that façade geometry fundamentally reshapes the energy-daylight-glare trade-off. Daylight saturation occurs at relatively low WWR depending on room geometry, and additional glazing provides minimal visual benefit while incurring disproportionate cooling penalties and glare. Energy loads increase non-linearly, with East and West orientations showing 234-329% escalation. Building aspect ratio determines which orientations dominate thermal performance. Benchmarking against China's and India's Eco Niwas Samita confirms alignment with regional guidelines. The findings are synthesized into geometry-aware design recommendations for contexts lacking energy regulations, including orientation-specific WWR limits.

Keywords: window-to-wall ratio, façade geometry, energy-daylight interaction, standardized regression coefficients

1. INTRODUCTION

1.1. Background

The building sector is the largest energy consuming sector globally, accounting for nearly one-third of the total energy consumption. This underscores the critical importance of improving building energy performance as a central strategy for energy conservation and climate change mitigation [1]. The energy consumed by the building sector also varies between developed and developing nations—while buildings in developed nations consume 20%-40% of the total energy [2], those in developing countries account for approximately 40% of the total energy use [3]. This highlights the universal significance of building energy efficiency and the need for intervention in developing countries.

Within this global context, Nepal presents a compelling case of urbanization driven energy challenges. According to the Water and Energy Commission Secretariat [4], 27.1% of Nepal's population resides in urban areas, 39.7% in peri-urban areas, and 33.2% in rural areas. This distribution of population is shifting rapidly due to accelerating urbanization, which in turn is increasing the energy demands in cities with high building density and energy-intensive

*Corresponding author.
prashantxytre@gmail.com (P. Chhetri)

Received 15 February 2026; Revised 9 April 2026; Accepted 18 May 2026; Published online 6 July 2026

Citation: Prashant Chhetri, Façade Geometry, Orientation, and Window-to-Wall Ratio: An integrated Energy and Daylight performance study for Kathmandu's temperate climate, Journal of Daylighting, 13:2 (2026) 363-377. doi: 10.15627/jd.2026.21

NOMENCLATURE

WWR	*Window-to-wall ratio*
SRCs	*Standardized regression coefficients*
WECS	*Water and energy commission secretariat*
sDA	*Spatial daylight autonomy*
sGA	*Spatial glare autonomy*
EUI	*End use intensity*
ACH	*Air changes per hour*
Cwb	*Koppen-geiger climate classification for temperate climates*
EPW	*Energy plus file*
TMY	*Typical meteorological year*
RCC	*Reinforced cement concrete*

lifestyles and the most energy intensive is the residential sector which dominates the national energy consumption at 60.59% [4], a share that far exceeds the global averages of 40%.

This situation is both a vulnerability and an opportunity for Nepal because the excessive demands can be reduced with improvements in the building design, particularly through the optimization of the fenestration which can reduce energy consumption by up to 40% depending on climatic conditions [5].

Windows are one of the crucial components of the building envelope system. They are not only required for aesthetic purposes but also for daylighting and proper thermal enclosure [5]. However, they are a major source of energy transfer; Amaral et al. [6] identifies windows as one of the biggest contributing factors for energy loss. Consequently, windows must be critically designed for energy efficiency purposes [1]. Alwetaishi [7] stresses that windows are one of the most fragile energy transfer systems and require a great deal of attention from engineers and architects.

The Window-to-Wall Ratio (WWR) is defined as the ratio of the area of the glazing to the exterior wall surface area, denoted by the equation where Sw is the area of the glazing and S_f is the area of the façade [1,5].

$$WWR = \frac{Sw}{Sf} \quad (1)$$

According to the ASHRAE Handbook of Fundamentals, Window-to-Wall Ratio affects occupant comfort and building energy use through the means of conduction, radiation, daylighting and infiltration. These impacts are dependent on a combination of variables, including the physical properties of the glazing such as the Solar Heat Gain Coefficient (SHGC), Visual Transmittance (Tv), and thermal conductance (U-value) and the local climatic conditions [5]. Beyond the physical properties, the size of the window or WWR and its Window Orientation (WO) are also equally important. Window Orientation dictates the amount of solar radiation a building's façade receives, which is one of the major factors driving the building's cooling load [8,9].

Research conducted worldwide gives us a broader perspective into the optimal values of WWR specific to the climatic location of those places. Goia [10], while studying for optimal WWR for different European climates found that the value regardless of the climate lies between 0.3 to 0.4, with energy use increasing by 5% to 25% when WWR was outside of the mentioned range. A simulation of 162 scenarios was done in China where it was concluded that the optimum Window-to-Wall Ratio is highly dependent on the building orientation, with southeast orientations performing the best overall. The recommended WWR was 35% for the most south facing walls and 40% for north facing walls [11]. A study conducted in the Yanqui library of Jimei university found the optimal values to be 55% for north and south facing rooms, 53% for east rooms, and 38% for west facing rooms [12]. In the local context, the studies for Kathmandu suggest a lower optimal range. Research indicates a minimum WWR of 0.24 is required for habitability and effective light distribution [13]. Another study corroborates WWR as a fundamental design parameter, concluding that 30% is the optimum WWR for energy use and achieving a target illuminance of 500 lux in office buildings. The authors emphasize that a window area beyond limits results in negative outcomes like overheating and excessive glare without improving the overall illuminance [14].

1.2. Sensitivity analysis

Sensitivity analysis is considered to be one of the most important tools in overall building energy simulation and energy analysis [15,16]. Research has shown that sensitivity analysis has been extensively and proactively used to examine and explore various parameters of building thermal performance. Sensitivity analysis helps in ranking the importance of input variables, which is crucial for optimizing building design and performance. For instance, the thermal transmittance and solar absorptance were identified as key variables affecting heating and cooling loads, respectively, in a study using different global sensitivity analysis methods [17]. Sensitivity analysis (SA) is also used to test and improve the building energy simulations, which is done by addressing uncertainties in various input parameters [18].

Sensitivity Analysis is mainly divided into three categories: 1) Screening method which is computation extensive and costly and 2) Local SA which is simple quantitative method—also known as one-parameter-at- a time (OTA) and can be done with low computational cost but with some limitations when interpreting non-linear relationships between inputs and outputs. To overcome these limitations 3. Global SA—which does a better job at interpreting such complex relationships is used [19]. Tian [15] (p. 412) provides us with a categorization and sub-categorization of Local and Global SA where Global SA is categorized based on three methods: Regression, Screen, Variance based Meta-model, which are further subtyped into SRC, SRRC, t-value, Morris, FAST, Sobol, MARS, ACOSSO, and SVM where Standard Regression Coefficient (SRC) is a type of Global SA and a subtype of Regression Method which is suitable for linear models. It is also one of the most common Global SA methods which based on Ordinary Root Square (ORS) [20]. A larger coefficient values denotes a larger impact,

https://dx.doi.org/10.15627/jd.2026.21

positive value denotes a positive impact and negative value denotes a negative impact in the case of SRCs [21].

The application of SRCs in building performance research has grown substantially in recent years. A study used Standardized Regression Coefficients (SRC) to quantify the sensitivity of various parameters, such as glass type and wall construction, to building costs and energy consumption. They provide a numerical representation of the strength and direction of relationships, facilitating effective comparison of impacts [22]. One study used Standard Regression Coefficients (SRCs) to determine the effect of Window-to-Wall Ratio (WWR) on energy performance compared to other variables such as daylighting [23].Similarly, studies done by Ayoub [24] and Fang and Cho [21] used SRCs to determine the relationship between different variables in the urban configuration.

1.3. Research gap

The preceding review establishes that Window-to-Wall Ratio (WWR) optimization has been extensively studied across diverse climates, with researchers identifying orientation dependent optimal ranges and developing sensitivity analysis methods to rank the importance of various design parameters. However, several gaps persist in the current body of knowledge specifically for Kathmandu. Very few studies have been done in regards with quantifying WWR with respect to Daylight and Glare. [14] did a case study which used outdated simulation model (Ecotect) and analyzed only Energy consumption and daylighting with no glare evaluation for an office building. Another similar study done by Awale and Uprety [25] focuses only on energy use without analyzing useful daylighting and glare. Very few studies that have been done regarding WWR optimization for Kathmandu. Similarly, no prior studies have been done to quantify the effect of paired façades in a room (i.e. how windows on adjacent sides of a room interact and effect the heating and cooling loads of a room).

This study aims to quantify the optimal WWR values for Kathmandu, where urbanization is rapid and there is a lack of proper energy regulatory framework. Second, it aims to quantify the interaction between paired façades in a room and how geometry of the façade determines the optimal Window-to-Wall Ratio.

2. METHODOLOGY

This research examines the relationship between energy use, WWR and orientation. The framework was divided into: (1) Collecting the room sizes from various available and constructed buildings. (2) Calculating mean length and width for Geometry Creation. (3) Running simulations for single façade and paired façades. (4) Conclusions on optimal WWR.

2.1. Geometric model creation

This first step of the study began by collecting room sizes data of 50 rooms in total built across the Kathmandu valley. The buildings were selected on the basis of construction materials used that is common to Kathmandu's building typology. The houses that were selected were constructed with Reinforced Cement Concrete (RCC), cement bonded brick walls, and RCC roof slabs, which represent the dominant residential construction typology in Kathmandu [26]. Table 1 presents the descriptive statistics of the surveyed geometries, and Fig. 1 shows the distribution of room lengths and widths. The mean dimensions (3.96m x 3.23m) L x B were used to create a single-zone "shoe-box" model for parametric simulation.

This geometric model attempts to replicate a single room of a residential building. Since the attempt is to analyze the effect of WWR and façade geometry in building energy, the façade is the only surface from which heat exchange occurs with the surrounding with other three walls, floor and the roof being adiabatic. This methodology of using a simple box model with all faces adiabatic except for the face with the window was adopted from the studies done by [27] and [3]. The parametric model was created using Grasshopper which is a parametric plug-in for the 3D designing software Rhinoceros 3D. The developed parametric model was simulated using Energy-plus and Radiance for energy analysis and daylighting analysis [27]. End Use intensity (EUI) kWh/m²/yr and Spatial Daylight Autonomy (sDA) were analyzed. Where, EUI represents the total amount of energy used for heating, cooling or total per year per m². sDA is defined as the percentage of floor area that receives at least 300 lux of daylight for at least 50% of the occupied hours [28]. Spatial Glare Autonomy used in the study was introduced by [29] where glare autonomy is a 40% GA40% threshold of Daylight Glare Probability (DGP) and Spatial Glare Autonomy is sGA40%,5% with a target of 5% of occupied hours. sGA is a metric that calculates the spatial distribution of glare and complements sDA which is also a spatial metric. Lower sGA values indicate higher spatial distribution of glare (i.e. Lower WWR have higher sGA values and lower sGA = more glare). The heating and cooling set points were 18°C and 26°C [30]. Building Program, Envelope material properties, Radiance Parameters are summarized in Table 2, Table 3, and Table 4.

The default radiance parameters provided by Ladybug v.1.8.0 were used for daylighting simulation.

2.2. Window construction

Nepal currently has no established national standards or guidelines for energy-efficient window glazing in buildings. Therefore, to ensure reproducibility and provide a consistent baseline for comparative analysis, this study employed the default window construction provided by the simulation tool (Honeybee Standards library).

The glazing assembly is the "Generic" construction, defined in the "energy_default.json" file of the Honeybee-standards repository with U-value of 0.59 W/m².K, SHGC of 0.36, and Tvis of 0.6. The same construction was applied uniformly across all model variations, including all orientations, wall configurations (short wall and long wall), and Window-to-Wall Ratios. This consistency

https://dx.doi.org/10.15627/jd.2026.21

Table 1. Descriptive Statistics for Length and Width of 50 surveyed Room Geometries.

	N	Minimum	Maximum	Mean	Std. deviation	Skewness	
Length (m)	50	2.69	5.49	3.9544	0.554908	0.777537	0.336601
Width (m)	50	2.21	3.96	3.2368	0.431662	-0.77887	0.336601

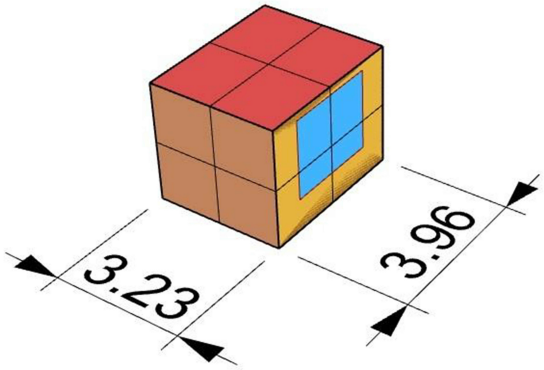

Fig. 1. Geometric model visualized in rhino 3D.

Table 2. Building program parameters for parametric simulations.

Attributes	Value
Project Type	Single Residential Room
Zones program	Midrise Apartment
People per area	0.078 m2
Metabolic rate	Metabolic rate of seated person
Equipment load	6.7 W/m2
Lighting Load	9.4 W/m2
ACH	0.5
Infiltration	0.000569 m3/s-m2
HVAC Template	HVAC ideal Air
Heating Setpoint Temperature	18
Cooling Setpoint Temperature	26

Table 3. Material properties for envelope construction, representing the dominant residential typology in Kathmandu.

Property	Units	9" Brick walls	Cement Plaster
Thickness	m	0.23	0.012
Conductivity	W/m.K	0.7	0.87
Density	Kg/m3	1800	2000
Specific Heat	J/kg.K	840	840

ensures that the comparative analysis of building form is not influenced by variations in envelope thermal.

2.3. Climatic data

Kathmandu lies at 27◦42′ N, 85◦22′ E representing the warm temperate climate of Nepal and according to Koeppen-Geiger Climate classification it falls under the "Cwb" region [31]. It is one of the cities inside Kathmandu Valley which comprises of Kathmandu, Bhaktapur and Lalitpur. The elevation ranges from 1,200 meters to 2,750 meters, which creates a diverse climatic condition within the valley [32]. The monthly climatic profile of the valley is illustrated in Fig. 2.

3. DATA ANALYSIS AND RESULTS

This study systematically investigates how façade geometry moderates the relationship between Window-to-Wall Ratio (WWR), orientation, and building performance. The results are organized in two stages: first, single-façade configurations establish the fundamental moderating role of geometry; second, paired-façade reshapes sensitivity hierarchies when multiple orientations interact and a total of 360 simulations were carried out.

Table 4. Daylight Simulation (Radiance) parameters.

Parameter	Values
Ambient Bounces (-ab)	2
Ambient Divisions (-ad)	5000
Limit Weight (-lw)	2e-05
Analysis grid spacing	0.2 m
Analysis height	0.8 m

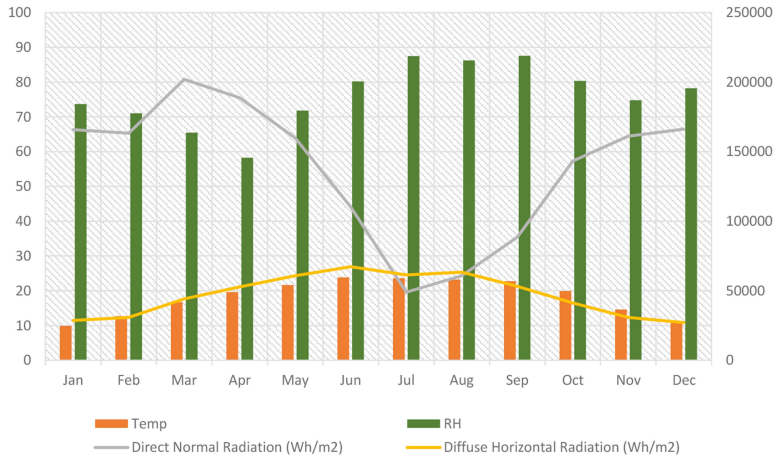

Fig. 2. Monthly Climatic profile of Kathmandu: temperature (°C) and precipitation (mm).

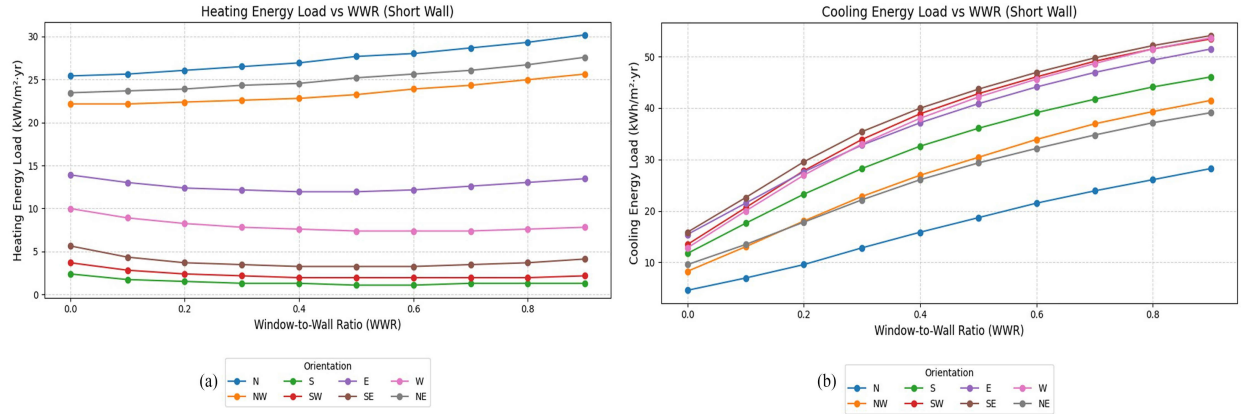

Fig. 3. Thermal performance of Scenario A: (a) heating load, (b) cooling load.

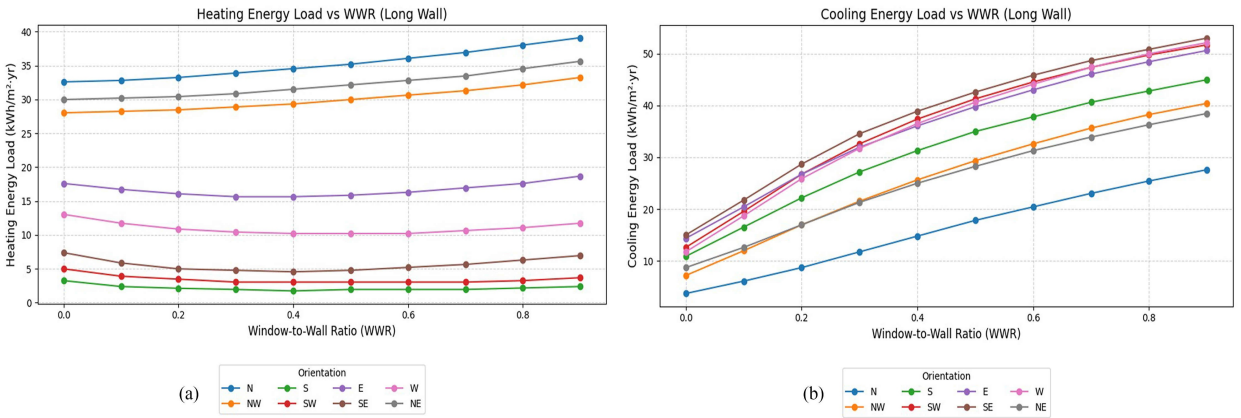

Fig. 4. Thermal performance of Scenario B: (a) heating load, (b) cooling load.

https://dx.doi.org/10.15627/jd.2026.21

3.1. Single façade analysis

The single-façade analysis compared two geometrically distinct scenarios derived from Kathmandu's residential building stock: Scenario A, with windows on the shorter wall (3.23 m width) and a deeper room (3.96 m depth); and Scenario B, with windows on the longer wall (3.96 m width) and a shallower room (3.23 m depth). This paired comparison isolates the effect of geometry while holding orientation and WWR constant which is a critical experimental design that reveals geometry's role not as a secondary variable but as a fundamental moderator of performance outcomes. A total of 160 simulations scenarios were run (8 orientations x 10 WWR values x 2 façade geometries), evaluating End Use Intensity (EUI) and Spatial Daylight Autonomy (sDA).

3.1.1. Thermal performance

Figures. 3 and 4 illustrate a consistent pattern: the same WWR and orientation produce fundamentally different energy outcomes depending solely on which wall hosts the window. In Scenario A (Short façade, deeper room depth), cooling loads exhibit exponential increases across all orientations as WWR progresses from 10% to 90% (**Fig. 3** (b)). East-facing windows show an increase from 15.42 to 51.47 kWh/m²/yr, which is an escalation of 234%, while West-facing windows show an even steeper 329% increase (12.81 to 53.64 kWh/m²/yr). These dramatic increases confirm that even modest glazing on East and West orientations carries significant cooling penalties. South-facing windows show a moderate increase from 11.73 to 46.04 kWh/m²/yr, while North-facing windows show the smallest absolute increase from 4.56 to 28.23 kWh/m²/yr. The exponential nature of these increases is evident in the progressive steepening of the cooling load curves as WWR increases.

Heating loads display the exact inverse relationship with solar exposure (Fig. 3 (a)). North-facing orientations, which receive minimal direct sun, increases the heating demand by 19% (25.63 to 30.19 kWh/m²/yr) as WWR increases. This confirms that larger north windows function as net heat loss devices. Conversely, South facing orientations reduce heating demand by 45% (2.39 to 1.30 kWh/m²/yr) over the same WWR range, validating the passive solar potential of south glazing when appropriately sized. Southeast and Southwest orientations show similar benefits, with 42% and 41% reductions respectively.

Scenario B (Long façade, shallow room) fundamentally shifts these relationships (Fig. 4(a) & Fig. 4(b)). Baseline heating loads are 28-30% higher across all orientations compared to Scenario A. For South orientation at 30% WWR, heating load is 1.96 kWh/m²/yr in Scenario B compared to 1.30 kWh/m²/yr in Scenario A. For North orientation at 30% WWR, heating load is 33.88 kWh/m²/yr in Scenario B compared to 26.50 kWh/m²/yr in Scenario A. This elevation is directly attributable to the larger absolute glazing area (approximately 23% more glass at the same WWR percentage) and the reduced thermal mass in shallower rooms, which limits passive heat storage during the day and increases heat loss at night.

Cooling penalties in Scenario B are similar in pattern to Scenario A, though with marginally lower absolute peak values due to reduced thermal mass. East orientation cooling increases by 253% from 10% to 90% WWR, reaching 50.60 kWh/m²/yr (compared to 51.47 in Scenario A). West orientation reaches 52.12 kWh/m²/yr at 90% WWR (compared to 53.64 in Scenario A). The slightly lower cooling peaks in Scenario B (approximately 2-3% lower) occur despite larger absolute glazing area (23% more glass at same WWR), indicating that the reduction in thermal mass in shallow rooms partially mitigates peak cooling loads by limiting heat storage and re-radiation.

3.1.2. Daylight, glare and energy trade-off analysis

The trade-off between daylight autonomy (sDA), spatial glare autonomy (sGA), and total EUI differs between the two geometric scenarios. Scenario A and Scenario B which represent two dominant residential configurations in Kathmandu. The analysis reveals that geometry not only shifts the optimal WWR range but also changes the nature of the trade-off between various metrics.

- **South orientation**
  For south-facing façades as shown in Fig. 5, Scenario B achieves higher sDA at lower WWR (0.938 vs 0.733 at 20% WWR) due to absolute larger window area and shallower room depth. However, this comes at the cost of worse glare performance (sGA = 0.368 vs 0.438 at 20%). Total EUI remains relatively same between scenarios at each WWR level. For scenario A the optimal balance point between glare and daylight is around 20-30% WWR, whereas, for the same WWR range, Scenario B produces excellent daylight but unacceptable glare (sGA = 0.247 at 30% WWR). This suggests that while some kind of shading might be required if visual comfort is the topmost priority.
- **West orientation**
  Out of all four cardinal directions, West orientation presents itself as the most challenging trade-off scenario due to afternoon sun exposure. Scenario B has overall higher total EUI by few points due to higher absolute glazing area (EUI = 40.82 kWh/m2/yr, WWR = 30% for Scenario A and EUI = 42.13 kWh/m2/yr, WWR = 30% for Scenario B) as shown Fig. 6 Scenario B achieves both higher sDA and higher sGA at 20% WWR (0.911 vs 0.743 for sDA; 0.569 vs 0.526 for sGA). This suggests that for west-facing rooms, the shallow configuration provides better daylight with less glare which can be seen in Fig. 6. This is the complete opposite to pattern observed for south orientation.

  The trade-off point for west orientation is more constrained than south. At 20% WWR, sGA is already borderline (0.526-0.569), and by 30% WWR, sGA drops to unacceptable levels (0.375-0.441) while total EUI increases by 15-17%. This indicates that west-facing rooms should maintain WWR at or below 20%, regardless of geometry.

https://dx.doi.org/10.15627/jd.2026.21

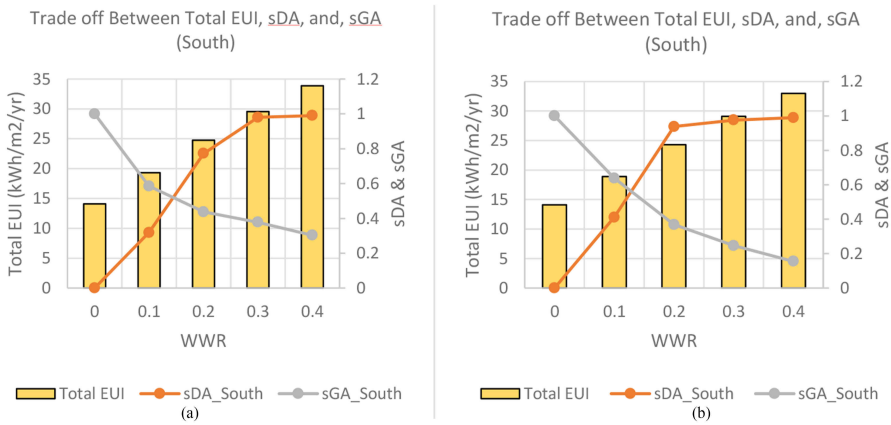

Fig. 5. Trade-off between EUI, sDA, and sGA. (a) Scenario A and (b) Scenario B for South Orientation.

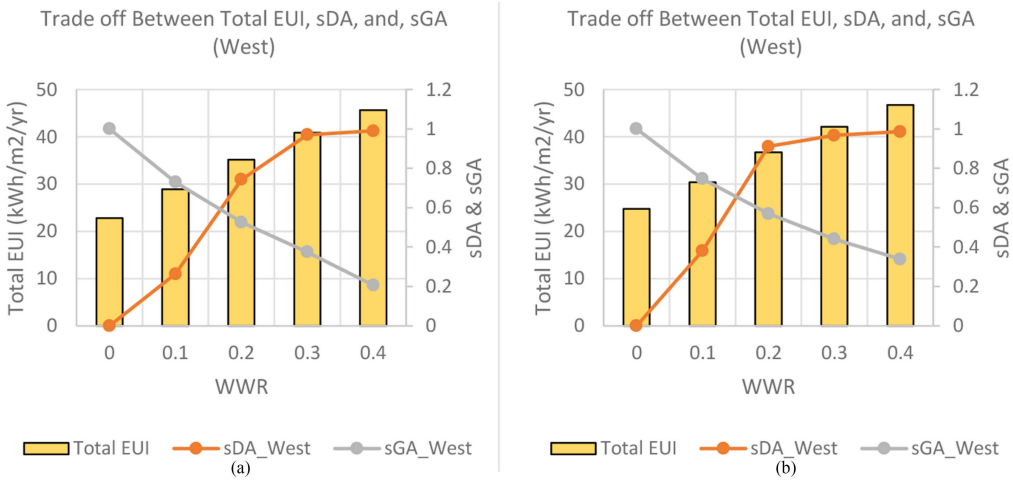

Fig. 6. Trade-off between EUI, sDA, and sGA. (a) Scenario A and (b) Scenario B for West Orientation.

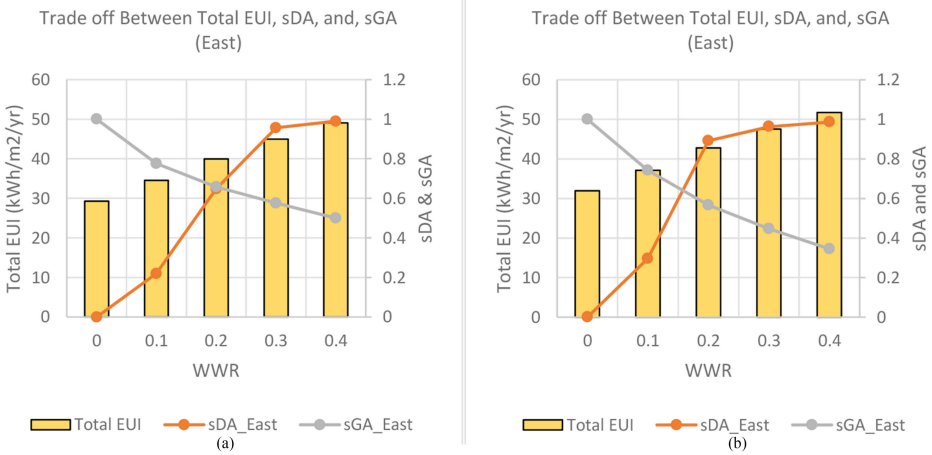

Fig. 7. Trade-off between EUI, sDA, and sGA. (a) Scenario A and (b) Scenario B for East Orientation.

- **East orientation**
  East orientation shows similar patterns to west but with less severe glare. Scenario A (deep room) achieves higher sGA at both WWR levels (0.658 vs 0.566 at 20%; 0.576 vs 0.447 at 30%), while Scenario B achieves higher sDA visualized in Fig. 7.

This represents a clear trade-off: designers must choose between better daylight (Scenario B) or better glare control (Scenario A).

https://dx.doi.org/10.15627/jd.2026.21

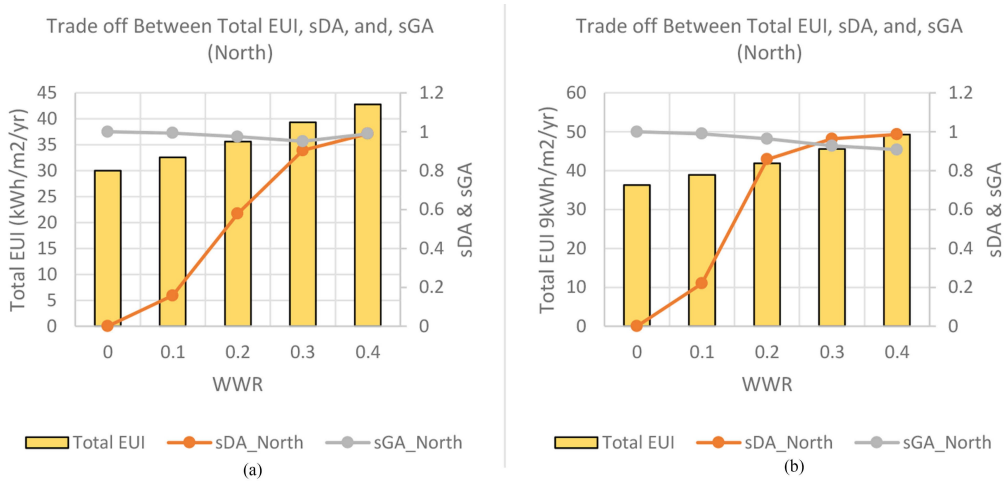

Fig. 8. Trade-off between EUI, sDA, and sGA. (a) Scenario A and (b) Scenario B for North Orientation.

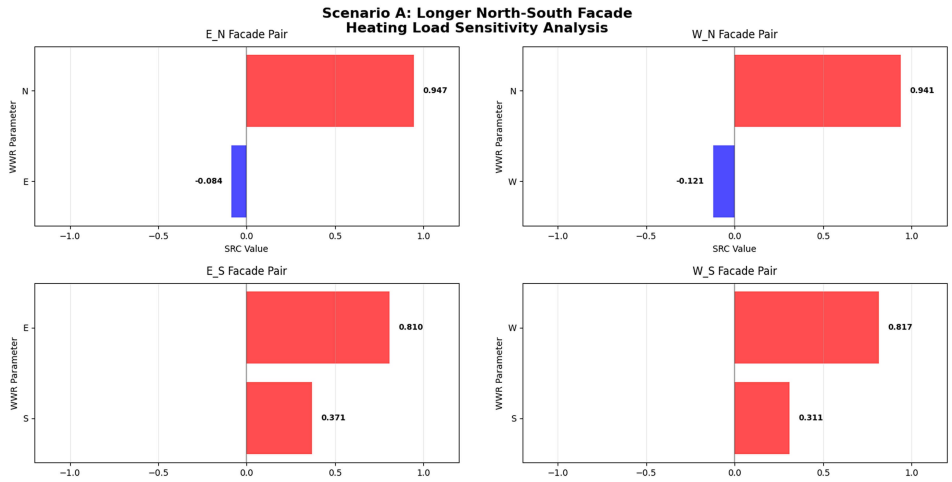

Fig. 9. Heating Load SRCs for Scenario A (Longer North-South Axis) of paired façade analysis.

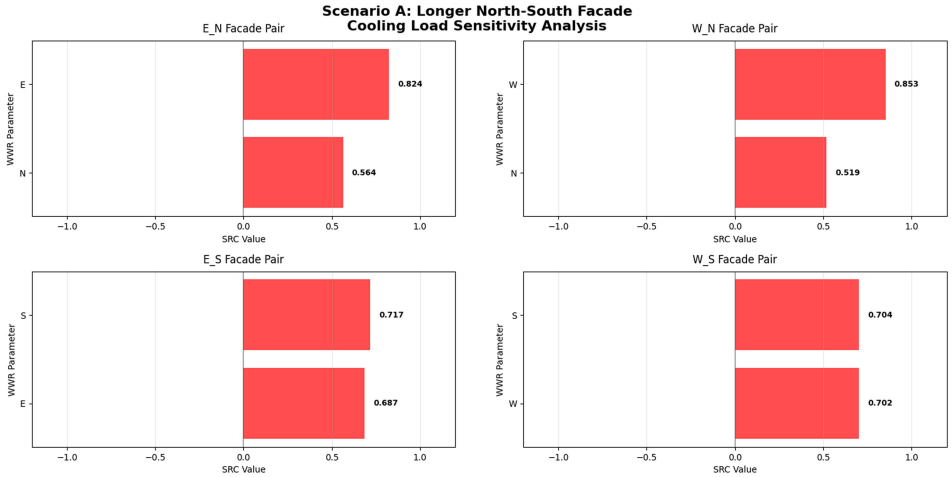

Fig. 10. Cooling Load SRCs for Scenario A (Longer North-South Axis) of paired façade analysis.

Total EUI is higher for Scenario B at all WWR levels (42.79 vs 39.96 at 20%), suggesting that deep rooms are more energy-efficient for east orientation.

- **North orientation**

  For north orientation, sGA remains excellent in both scenarios (>0.92 at all WWR). The primary trade-off is between daylight and energy. Scenario B achieves higher sDA at lower WWR (0.858 vs 0.579 at 20%) but with higher total EUI (41.92 vs 35.62)

https://dx.doi.org/10.15627/jd.2026.21

visualized in Fig. 8. Scenario A achieves daylight targets at 30% WWR (0.904) with lower energy costs.

Key insights that emerge from this analysis are: Shallow rooms (Scenario B) achieve targets at lower WWR for all orientations due to reduced depths. However, this benefit is offset by worse glare performance for south orientation and higher total EUI for east and north orientations. Deep rooms (Scenario A) provide more design flexibility because the trade-off between daylight and glare is less abrupt, whereas shallow room shows rapid sDA saturation and intense glare. East and West orientations, especially West should be prioritized the most for glare mitigation strategies because at just 20% WWR, sGA is already at (0.526-0.569), and total EUI increases by 15-17% from 20% to 30% WWR depending on the scenario.

3.1.3. Benchmarking against regional guidelines

To contextualize these findings against established regulatory benchmarks, key parameters were compared with China's GB 55015-2021 for Hot Summer Cold Winter (HSCW) zone [33] and India's Eco Niwas Samita (ENS) [34] whose climate is similar to Kathmandu's temperate conditions. The code mandates stricter WWR limits for East and West façades (0.24, 0.25) compared to south (0.35-0.4), and WWR of 0.27 for North while having a constant Tvis of 0.6 across all scenarios. Similarly, India's ENS for prescribes a (20-30%) as the minimum WWR for East and West façade and provides < 30% WWR for South façade. ENS states high WWR acceptable for North due to low exposure to direct solar radiation but caution should be taken as the above analysis shows Northern façades have the highest heat loss (Fig. 4 and Fig. 5). This comparison, while not validation, supports the above analysis and shows that WWR lies at a similar range for similar regional climatic contexts.

3.2. Paired façade analysis

The paired façade analysis extends the single façade findings by examining interactive energy effects of WWR combinations across paired façades and a total of 200 simulations were run. Similar to Single façade analysis, this section also examines two scenarios: 1) Scenario A with elongated North-South axis and 2) Scenario B with elongated East-West axis. Opposing façade configurations were excluded to reflect typical residential rooms.

3.2.1. Scenario A

In rooms where the North-South axis is longer, Heating load sensitivity is dominated by the longer North and South façades Fig. 9. In North-East combinations, the North façade dominates (SRC = 0.947) with minimal East influence (SRC = -0.084). Similarly, in North-West combinations, North dominance persists (SRC = 0.941) with West façades showing slight negative influence (SRC = -0.121) indicating that West glazing actually reduces heating demand slightly through afternoon solar gain, though at the cost of substantial cooling penalties.

Cooling load sensitivity tells a different story Fig. 10. In North-East combinations, the East façade (SRC = 0.824) substantially outweighs the North (SRC = 0.564), reflecting the disproportionate impact of morning solar gain on cooling loads. North-West combinations show even stronger West dominance (SRC = 0.853) compared to North (SRC = 0.519), confirming afternoon sun as a critical overheating driver.

The South-East and South-West combinations reveal the most complex trade-offs. For heating, East (SRC = 0.810) and West (SRC = 0.817) dominate over South (0.371 and 0.311 respectively), a finding that challenges the conventional emphasis on South-facing passive solar design. For cooling, however, both orientations in each pair show nearly equal influence (South-East: SRC_south = 0.717, SRC_east = 0.687; South-West: SRC_west = 0.717, SRC_south = 0.687), creating genuine design dilemma where passive heating benefits must be balanced against overheating risks.

Figure. 11 visualizes the total EUI for Scenario A as a heatmap. This can be used as a visual aid by architects', engineers, and designers to visually figure out optimal WWR for paired façades for real world design cases emulating Scenario A i.e. Longer North-South axis. Dark blue regions represent the lowest sum total of heating and cooling load whereas bright yellow represents the highest sum total of heating and cooling load for four different configurations analyzed in Scenario A.

3.2.2. Scenario B

When room geometry shifts to elongation along the East-West axis, the thermal hierarchy undergoes a fundamental re-orientation Fig. 12 and 13. The longer East and West façades become overwhelmingly dominant, while North and South orientations shift to secondary roles.

In North-East combinations, heating loads maintain strong North influence (SRC = 0.915) with modest East contribution (SRC = 0.100). But cooling loads tell the decisive story: extreme East dominance (SRC = 0.902) with moderate North influence (SRC = 0.420). The elongated East façade amplifies morning solar gain, making it the primary driver of cooling demand regardless of North glazing. North-West combinations mirror this pattern. Heating shows North dominance (SRC = 0.914) with negligible West impact (SRC = 0.066). Cooling, however, exhibits strong West dominance (SRC = 0.908) with moderate North contribution (SRC = 0.412). The extended West elevation transforms afternoon sun into the dominant cooling load determinant.

South-East and South-West combinations show the most dramatic hierarchy shift. Unlike Scenario A, where South moderated East/West impacts, here East and West dominate both heating and cooling (SRCs ~0.8), with South façades showing minimal heating impact and moderated cooling influence.

https://dx.doi.org/10.15627/jd.2026.21

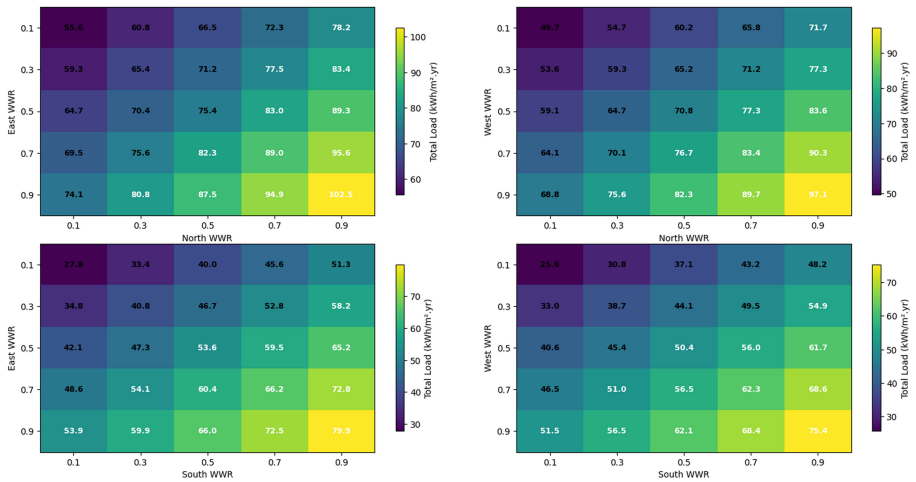

Fig. 11. Heatmaps of total EUI for all 4 configurations analyzed in Scenario A.

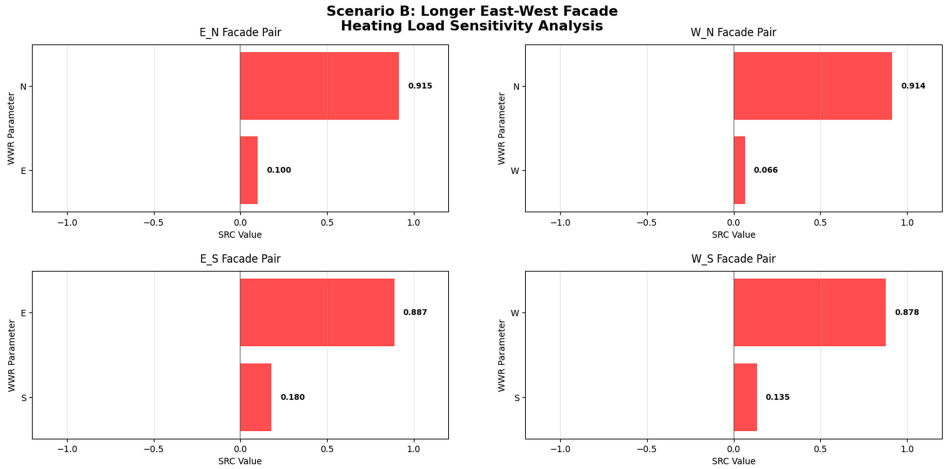

Fig. 12. Heating Load SRCs for Scenario B (Longer East-West Axis) of paired façade analysis.

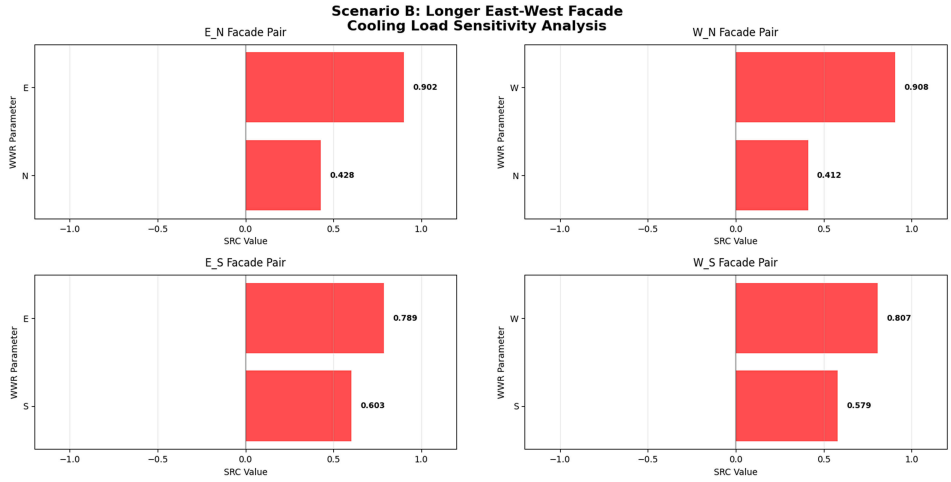

Fig. 13. Cooling Load SRCs for Scenario B (Longer East-West Axis) of paired façade analysis.

The geometric elongation effectively "amplifies" the solar exposure of East and West orientations, making them the primary thermal drivers regardless of which adjacent orientation accompanies them.

Similar to Fig. 11, Fig. 14 also provides a comprehensive visualization of total energy loads across WWR combinations in the longer East-West axis configuration with dark blue representing lower total value and yellow representing the higher total values.

https://dx.doi.org/10.15627/jd.2026.21

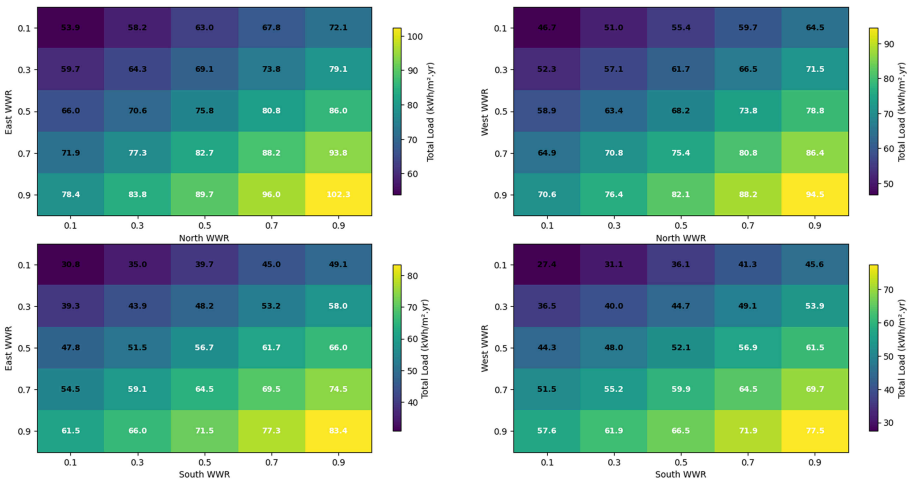

Fig. 14. Energy performance heatmaps for Scenario B.

Table 5. Coefficient of determination, adjusted coefficient of determination and variance inflation factor of paired façades.

Scenario	Load Type	Façade Pair	R^2	Adjusted R^2	VIF
A	Heating	E_N	0.904	0.896	1
A	Heating	W_N	0.899	0.89	1
A	Heating	E_S	0.794	0.776	1
A	Heating	W_S	0.764	0.743	1
A	Cooling	E_N	0.998	0.998	1
A	Cooling	W_N	0.997	0.996	1
A	Cooling	E_S	0.985	0.984	1
A	Cooling	W_S	0.988	0.987	1
B	Heating	E_N	0.848	0.834	1
B	Heating	W_N	0.84	0.825	1
B	Heating	E_S	0.819	0.802	1
B	Heating	W_S	0.789	0.77	1
B	Cooling	E_N	0.996	0.996	1
B	Cooling	W_N	0.994	0.993	1
B	Cooling	E_S	0.986	0.985	1
B	Cooling	W_S	0.987	0.986	1

The paired-façade SRC analysis yields a critical insight with direct design implications: building massing and plan proportion predetermine which orientations will be most consequential for energy performance. This finding elevates geometry from a passive context variable to an active determinant of design strategy. In North-South elongated forms, the classic orientation hierarchy holds: North drives heating, South enables passive gains, East/West create asymmetric cooling risks. Design can prioritize shading on East/West while optimizing South glazing. In East-West elongated forms, the hierarchy is overturned: East and West become the dominant drivers of both heating and cooling, with North and South relegated to secondary roles. Design must prioritize extreme solar control on the long East and West façades, treating glazing on these orientations as the primary energy variable regardless of adjacent orientations.

3.3. Model diagnostics

3.3.1. Regression diagnostics

To assess the validity of linear assumptions underlying SRCs, comprehensive diagnostics were performed on all the regression models. Table 5 presents the diagnostic summary for all 16 configurations using IBM SPSS.

Variance Inflation Factor (VIF) analysis confirms no multicollinearity issues (VIF = 1.0 for all models), as WWR on opposing façades were varied independently during simulation design. This ensures that SRCs reliably reflect parameter importance without confounding from correlated predictors.

Model fit (R^2) ranges from 0.764 to 0.998 across all configurations, with a mean of 0.912. Heating load models show slightly lower but still strong fit (mean R^2 = 0.841), while cooling load models exhibit near perfect fit (mean R^2 = 0.992). These values indicate that linear models capture the highest majority of variance

in energy outcomes, despite the presence of curvature in the underlying relationships.

3.3.2. Spearman's rank correlation for monotonic relationship validity

To validate that SRCs provide reliable parameter rankings despite non-linearity, Spearman's rank correlation was performed on four representative configurations selected at random (Heating W-N, Cooling E-N) from Scenario A and (Heating E-S and Cooling W-S) from Scenario B. For Scenario A, Heating W-N showed a strong monotonic relationship for WWR_N ($\rho = 0.952$, $p < 0.01$), whereas, WWR_W showed no significance ($\rho = -0.116$, $p = 0.000$); Cooling E-N showed strong positive monotonic relationship for WWR_E ($\rho = 0.832$, $p < 0.01$) and WWR_N ($\rho = 0.541$, $p < 0.01$). For Scenario B, Heating E-S showed strong positive monotonic relationship for WWR_E ($\rho = 0.922$, $p < 0.01$) while WWR_S showed no significant correlation ($\rho = 0.094$, $p < 0.654$); Cooling W-S showed strong positive monotonic relationships for both WWR_W ($\rho = 0.814$, $p < 0.01$) and WWR_S ($\rho = 0.567$, $p < 0.01$). Across all representative configurations, the dominant parameters identified by SRC showed strong, monotonic correlations, while non-dominant parameters showed weak or non-significant correlations. This perfect agreement between SRC rankings and Spearman correlations confirms the reliability of SRC for non-linear monotonic relationships.

4. DISCUSSIONS AND CONCLUSIONS

4.1. Discussions

The results demonstrate that façade geometry acts as a moderator for the relationship between WWR, orientation, and building performance in Kathmandu's temperate climate. This aligns with the findings made by Vanhoutteghem et al. [35] and Susorova et al. [36] Optimal WWR ranges differ by around 10% points between deep and shallow rooms despite the overall room geometry being constant. This is mainly driven by absolute glazing area being 23% more for the longer façade in the simulated geometric model and room depth governing the daylight penetration distance. A longer façade at 30% WWR results in a significantly larger window surface than a shorter façade at the same ratio. This directly escalates conductive heat transfer (U-value effects) and solar aperture (SHGC effects), explaining the 28-30% higher baseline heating loads in Scenario B. The non-linear, often exponential, rise in cooling loads across all orientations is therefore not merely a function of WWR proportion, but of absolute solar gain intensity, which is geometry dependent. This aligns with the broader understanding of windows as critical yet fragile thermal components [6,7]. Windows showed early daylight sufficiency at lower WWR, beyond which additional glare and heat penalties incurred. Similar observations regarding early daylight sufficiency at relatively low WWR and the importance of controlled glare through glazing properties and window placement have been reported by [37] for residential building.

Cooling loads escalate at an accelerating rate on East and West orientations. Studies done in the northern hemisphere corroborate with this finding. Feng et al. [38] states that East and West facing windows receive the strongest low angle solar irradiation; low WWR (10-20%) give lowest total energy and larger ratios quickly increase the cooling demands. Similarly, Cui et al. [39] in their study point South as the most stable orientation; minimal to no windows on West due to its volatility which is similar to the finding of this study. This finding is particularly important because cooling load is an increasing source of electricity demand, especially in developing countries [40]. For Kathmandu, where rapid urbanization and increasing adoption of energy intensive lifestyles are driving up the cooling demand, the results underscore the need for proper guidelines for façade designs. Glare is inevitable even at lower WWR for all orientations except North in both Scenarios (Section 3.1.2), so designers should prioritize what's most important: is it daylighting? Or is it Energy efficiency? and how much glare are they willing to admit into the geometry. Trade-offs are inevitable in window design process. Bagheri et al. [41] in their study for Rashat, Iran stated that larger WWR (≈54–58 %) can be provided because the benefits outweighed the extra heat gain due to larger windows. Another study by Sherif et al. [42] states that high WWR achieved highest sDA but in return elevated glare values exceeding the discomfort threshold and trade-offs were done to maintain glare at acceptable threshold while maintaining daylight sufficiency. So, designers and practitioners should make informed decisions on how trade-off occurs between WWRs and different orientations especially in places like Kathmandu where there is a lack of proper framework for energy efficient design of buildings in general.

SRC analysis reveals a shift in thermal hierarchy depending on the geometry of the model. In Scenario A (Elongated North-South axis) in paired façade analysis, it follows the North as source of heat loss and South as a source of heat gain dichotomy. But, when the form changes from North-South elongated to East-West elongated (Scenario B), the thermal hierarchies shift and East and West façade act as the primary drivers of both heating and cooling loads, overshadowing the influence of North and South façades. This finding implies the geometry of façades determine which façade will dominate the thermal performance. The application of SRCs to unravel such complex, interactive relationships between form and performance variables is supported by prior methodological work [21,24]. Spearman correlation was used to validate that the dominant WWR energy relationships are strongly monotonic ($\rho = 0.814$-0.952, $p < 0.01$) in nature and SRC—despite the non-linearity of the parameters—captures the ranking of parameters with high coefficient of determination. This method of validation of using Spearman correlation for non-linear and monotonic relationship is supported by Van Den Heuvel and Zhan [43] who

states Spearman's rank as more appropriate for non-linear monotonic relationships.

4.2. Conclusion

This research demonstrates that façade geometry acts as a moderator with absolute glazing area and room depth governing both thermal and luminous outcomes. Cooling loads escalate non-linearly on all orientations, with West facing façades showing the most critical energy and glare penalties as a whole regardless of the room geometry. Daylight Sufficiency is achieved at relatively low WWR (20% to 40%) for all orientations, beyond which additional glazing provides diminishing daylight returns with increased energy penalties and glare risk. The SRC analysis reveals that model form determines which orientation dominates thermal performance. In North-South elongated forms, North and South façades drive heating and cooling respectively. In East-West elongated forms, East and West façades become the primary thermal drivers, overshadowing North and South influences. Within the scope of this study (single-zone model, fixed glazing properties, two room configurations, and Kathmandu's Cwb climate), the findings offer preliminary guidance for climate-responsive façade design. Architects and engineers may adapt the proposed WWR ranges (≤ 20% for West, 20-30% for East and North, 30-40% for South with shading) while considering project-specific conditions. The design recommendations presented in Section 4.3 are intended as reference points rather than prescriptive rules.

4.3. General design recommendations

Several design recommendations were derived from the findings of this study that could extend beyond Kathmandu and could be applicable for places with similar climates which lack proper regulatory framework for efficient façade designs:

- West orientation is the most critical and regardless of the room depth and façade geometry, WWR for west should be minimal at around 20%.
- South orientation is stable and offers more design flexibility and can accommodate higher WWR; the passive solar gain may outweigh probable glare and a relative increase in EUI. Shading is recommended for WWR beyond 30%.
- North facing windows do not need constraints for glare but high WWR is not recommended due to higher heat loss.
- Building forms should be prioritized. In East-West elongated buildings the findings from a shoe-box model may carry over to a larger building with East and West being the dominant drivers for thermal loads.
- Daylight sufficiency is achieved at relatively low WWR, designers should explicitly prioritize which performance metric is most important for each project (daylight, energy efficiency, or visual comfort) and accept trade-offs accordingly. For orientations except North, some form of shading is recommended.

4.4. Contribution to theory and practice

This study extends the existing literature by quantifying how different façade geometry for same WWR and orientation effect the heating and cooling loads. Methodologically, this study advances the existing body of knowledge regarding the use of Standardized Regression Coefficients (SRCs) under monotonic and non-linear conditions through the combination of coefficient of determinations, VIF analysis and Spearman correlation (ρ = 0.814-0.952, $p < 0.01$), providing a replicable framework for the analysis of monotonic but non-linear relationships. This study also extends the existing body of knowledge for Kathmandu where previous studies did not focus on the trade-offs between energy, daylight and glare optimization for residential building stock and also quantifies how paired façades behave under different geometric forms and orientation. Finally, this study provides the quantification of geometry dependent WWR ranges for Kathmandu's residential building stock, providing evidence-based façade design guidelines for Kathmandu which could be applicable to similar climatic regions.

4.5. Limitation

While this research provides robust, evidence-based insights into the interplay between façade geometry, orientation, and Window-to-Wall Ratio (WWR) in Kathmandu's climate, several methodological and contextual limitations must be acknowledged. The study is performed on a simplified, single-zone "shoebox" model which, while widely adopted in parametric performance studies, does not fully replicate the complexities of real-world buildings such as inter-zonal heat transfer, thermal bridging, and multi-story dynamics. The analysis also does not account for adjacent structures, vegetation, or terrain that would cast shadows on the façade, which is an important factor in Kathmandu's dense urban fabric where mutual shading can significantly reduce solar heat gain, particularly on lower floors. Field Validation was not carried out due to lack of resources. Additionally, the study uses a Typical Meteorological Year (TMY) file based on historical climate data (2009-2023) and does not account for projected effects of climate change. Other limitations include fixed glazing properties, the absence of occupant behavior such as blinds or curtains, and the geometric analysis being limited to two room configurations. Despite these limitations, the relative patterns observed, including geometry effects, orientation hierarchies, and monotonic relationships, are likely robust as they are grounded in fundamental building physics and consistently observed across both geometric scenarios. Future research should employ climate projection files, multi-zone models, Field Validation, Multi-Objective Optimizations for clear trade-off analysis and a wider range of room proportions to extend these findings.

https://dx.doi.org/10.15627/jd.2026.21

FUNDING

This research received no external funding.

AUTHOR CONTRIBUTIONS

The author confirms being the sole contributor of this work and has approved it for publication.

ACKNOWLEDGEMENT

The author would like to thank his family and friends for their support throughout this research. During the preparation of this work, the author used DeepSeek in order to improve language and readability. After using this tool, the author reviewed and edited the content as needed and takes full responsibility for the content of the publication.

DECLARATION OF COMPETING INTEREST

The author declares no conflicts of interest.

REFERENCES

[1] C. Marino, A. Nucara, M. Pietrafesa, Does window-to-wall ratio have a significant effect on the energy consumption of buildings? A parametric analysis in Italian climate conditions, J. Build. Eng., 13 (2017) 169-183.
[2] L. Pérez-Lombard, J. Ortiz, C. Pout, A review on buildings energy consumption information, Energy Build., 40:3 (2008) 394-398.
[3] S. K. Alghoul, H. G. Rijabo, M. E. Mashena, Energy consumption in buildings: A correlation for the influence of window to wall ratio and window orientation in Tripoli, Libya, J. Build. Eng., 11 (2017) 82-86.
[4] Water and Energy Commission Secretariat, ENERGY SECTOR SYNOPSIS REPORT 2024, Water and Energy Commission Secretariat, 2024. [Online]. Available: https://wecs.gov.np/content/56/energy-sector-synopsis-report-2024--fy-2079-80-/
[5] L. Troup, R. Phillips, M. J. Eckelman, D. Fannon, Effect of window-to-wall ratio on measured energy consumption in US office buildings, Energy Build., 203 (2019) 109434.
[6] A. R. Amaral, E. Rodrigues, A. R. Gaspar, Á. Gomes, A thermal performance parametric study of window type, orientation, size and shadowing effect, Sustain. Cities Soc., 26 (2016) 456-465.
[7] M. Alwetaishi, Impact of glazing to wall ratio in various climatic regions: A case study, J. King Saud Univ. - Eng. Sci., 31:1 (2019) 6-18.
[8] A. Gasparella, G. Pernigotto, F. Cappelletti, P. Romagnoni, P. Baggio, Analysis and modelling of window and glazing systems energy performance for a well insulated residential building, Energy Build., 43:4 (2011) 1030-1037.
[9] M. Alshayeb, H. Mohamed, J. D. Chang, Energy Analysis of Health Center Facilities in Saudi Arabia: Influence of Building Orientation, Shading Devices, and Roof Solar Reflectance, Procedia Eng., 118 (2015) 827-832.
[10] F. Goia, Search for the optimal window-to-wall ratio in office buildings in different European climates and the implications on total energy saving potential, Sol. Energy, 132 (2016) 467-492.
[11] F. Chi, Y. Wang, R. Wang, G. Li, C. Peng, An investigation of optimal window-to-wall ratio based on changes in building orientations for traditional dwellings, Sol. Energy, 195 (2020) 64-81.
[12] V. Cheng, E. Ng, B. Givoni, Effect of envelope colour and thermal mass on indoor temperatures in hot humid climate, Sol. Energy, 78:4 (2005) 528-534.
[13] B. Sangraula, S. Uprety, Window to wall ratio for day lighting in context of apartment building in Kathmandu Valley, 1 (2020) 08-14.
[14] B. Basnet, S. Uprety, Daylighting in energy efficiency: a case of office building in Kathmandu, in: 12th IOE Graduate Conference, 2022, pp. 120-127.
[15] W. Tian, A review of sensitivity analysis methods in building energy analysis, Renew. Sustain. Energy Rev., 20 (2013) 411-419.
[16] R. Roka, A. Figueiredo, A. Vieira, C. Cardoso, A Systematic Review of Sensitivity Analysis in Building Energy Modeling: Key Factors Influencing Building Thermal Energy Performance, Energies, 18:9 (2025) 2375.
[17] R. Reitberger, F. Banihashemi, W. Lang, Sensitivity and Uncertainty Analysis of Combined Building Energy Simulation and Life Cycle Assessment, Implications for the Early Urban Design Process, in: CAADRIA 2022: Post-Carbon, Sydney, Australia, 2022, pp. 629-638.
[18] A. S. Silva, E. Ghisi, Evaluation of capabilities of different global sensitivity analysis techniques for building energy simulation: experiment on design variables, Ambiente Construído, 21:2 (2021) 89-111.
[19] S. Liu, Y. T. Kwok, K. K.-L. Lau, W. Ouyang, E. Ng, Effectiveness of passive design strategies in responding to future climate change for residential buildings in hot and humid Hong Kong, Energy Build., 228 (2020) 110469.
[20] A. S. Allam, H. A. Bassioni, W. Kamel, M. Ayoub, Estimating the standardized regression coefficients of design variables in daylighting and energy performance of buildings in the face of multicollinearity, Sol. Energy, 211 (2020) 1184-1193.
[21] Y. Fang, S. Cho, Design optimization of building geometry and fenestration for daylighting and energy performance, Sol. Energy, 191 (2019) 7-18.
[22] A. Asgari Motlagh, S. Havaeji, M. Orangian, A. Samadani, Achieving Net-Zero Energy Buildings: Analyzing and Optimizing Strategies Using Sensitivity Analysis, J. Asian Energy Stud., 8 (2024) 51-67.
[23] L.-G. Maltais, L. Gosselin, Daylighting "energy and comfort" performance in office buildings: Sensitivity analysis, metamodel and pareto front, J. Build. Eng., 14 (2017) 61-72.
[24] M. Ayoub, A multivariate regression to predict daylighting and energy consumption of residential buildings within hybrid settlements in hot-desert climates, Indoor Built Environ., 28:6 (2019) 848-866.
[25] A. Awale, S. Uprety, Impact of Window-Wall Ratio on Heating and Cooling Energy Consumption: A Case of Office Building in Kathmandu, in: Proceedings of 10th IOE Graduate Conference, Oct. 2021.
[26] National Statistics Office, National Population and Housing Census 2021 Provincial Report (BAGMATI PROVINCE), National Statistics Office, 2021.
[27] M. Mahdavinejad et al., The impact of facade geometry on visual comfort and energy consumption in an office building in different climates, Energy Rep., 11 (2024) 1-17.
[28] S. V. Ershov, V. G. Sokolov, A. G. Voloboy, V. A. Galaktionov, Effective Simulation of Spatial Daylight Autonomy and Annual Sunlight Exposure, in: Proceedings of the 32nd International Conference on Computer Graphics and Vision, Keldysh Institute of Applied Mathematics, 2022, pp. 64-72.
[29] N. L. Jones, Fast Climate-Based Glare Analysis and Spatial Mapping, in: Building Simulation 2019, Rome, Italy, pp. 982-989.
[30] S. Paudyal, S. B. Bajracharya, Energy efficiency in corporate building through envelop improvement, a case of Prabhu Bank Corporate building in Kathmandu, in: 6th IOE Graduate Conference, 2019.
[31] S. Bodach, W. Lang, J. Hamhaber, Climate responsive building design strategies of vernacular architecture in Nepal, Energy Build., 81 (2014) 227-242.
[32] S. Phuyal, Precipitation in Kathmandu Valley: A Spatial-temporal Study, Int. J. Environ. Clim. Change, 14:9 (2024) 266-278.
[33] X. Meng, Y. Meng, J. Nunoshige, Theoretical energy-saving potential assessment of an office building renovated to comply with GB 55015-2021 across three China climate zones, in: 2025 Building Simulation Conference, Aug. 2025.
[34] MoEF&CC, PASSIVE & LOW ENERGY COOLING STRATEGIES FOR ACHIEVING THERMAL COMFORT IN INDIA'S UPCOMING AFFORDABLE HOUSING, Ministry of Environment, Forest & Climate Change, 2022.
[35] L. Vanhoutteghem, G. C. J. Skarning, C. A. Hviid, S. Svendsen, Impact of façade window design on energy, daylighting and thermal comfort in nearly zero-energy houses, Energy Build., 102 (2015) 149-156.
[36] I. Susorova, M. Tabibzadeh, A. Rahman, H. L. Clack, M. Elnimeiri, The effect of geometry factors on fenestration energy performance and energy savings in office buildings, Energy Build., 57 (2013) 6-13.
[37] K. Kalaimathy, R. Shanthi Priya, P. Rajagopal, C. Pradeepa, R. Senthil, Daylight performance analysis of a residential building in a tropical climate, Energy Nexus, 11 (2023) 100226.
[38] G. Feng, D. Chi, X. Xu, B. Dou, Y. Sun, Y. Fu, Study on the Influence of Window-wall Ratio on the Energy Consumption of Nearly Zero Energy Buildings, Procedia Eng., 205 (2017) 730-737.

[39] X. Cui, S. Yin, L. Zhang, Y. Zhu, G. Sang, Q. Zhao, Influence Mechanism of Window-to-Wall Ratio on Energy Consumption of Rural Buildings in Southern Shaanxi, China, Int. J. Heat Technol., 37:2 (2019) 562-568.
[40] EA, World Energy Outlook 2025, Paris, 2025. [Online]. Available: https://www.iea.org/reports/world-energy-outlook-2025
[41] S. Bagheri, H. Moradinasab, M. Yeganeh, The effect of window proportions in low-rise residential buildings on annual energy consumption in humid temperate climate (case study: Rasht city in Iran), Front. Energy Res., 12 (2024) 1463678.
[42] N. Sherif, A. Yehia, W. S. E. Ismaeel, Simulation and Statistical Validation Method for Evaluating Daylighting Performance in Hot Climates, Urban Sci., 9:8 (2025) 303.
[43] E. Van Den Heuvel, Z. Zhan, Myths About Linear and Monotonic Associations: Pearson's r, Spearman's ρ, and Kendall's τ, Am. Stat., 76:1 (2022) 44-52.